

These findings provide evidence that cerebral processing operates dynamically in a distributed manner as in other vertebrate and invertebrate motor systems (11).

The finding that neurons coarsely encode a given parameter also supports a distributed organization. Individual neurons cannot accurately encode individual parameters, and this condition has generated population theories in which many neurons participate simultaneously. The resolution of the population code is better than a comparable code composed of individual neurons with narrow, discrete tuning. Coarse coding also makes it possible for a cell to encode more than one parameter simultaneously. Thus, a given neuron can participate in multiple populations representing different parameters.

REFERENCES AND NOTES

1. A. P. Georgopoulos, J. F. Kalaska, R. Caminiti, J. T. Massey, *J. Neurosci.* 2, 1527 (1982).
2. A. P. Georgopoulos, R. Caminiti, J. F. Kalaska, J. T. Massey, *Exp. Brain Res. Suppl.* 7, 327 (1983).
3. A. P. Georgopoulos, J. T. Lurito, M. Petrides, A. B. Schwartz, J. T. Massey, *Science* 243, 234 (1989).
4. A. B. Schwartz, *J. Neurophysiol.* 70, 28 (1993).
5. F. Lacquaniti, C. Terzuolo, P. Viviani, *Acta Psychol.* 54, 115 (1983). The exact value of the exponent may vary with overall speed [J. Wann, I. Nimmo-Smith, A. M. Wing, *J. Exp. Psychol. Hum. Percept. Perform.* 14, 622 (1988)] or in development [P. Viviani and R. Schneider, *J. Exp. Psychol.* 17, 198 (1991)] where a stable value of % is not reached until the age of 12. This law has been shown to be valid in a wide range of arm and drawing movements.
6. An experiment performed under isometric conditions in which subjects exerted force on a stationary handle to produce closed figures such as ellipses and lemniscates showed that this law was not the result of mechanical properties of the arm, because the law was valid when no displacement occurred [J. T. Massey, J. T. Lurito, G. Pellizer, A. P. Georgopoulos, *Exp. Brain Res.* 88, 685 (1992)].
7. A. B. Schwartz, *J. Neurophysiol.* 68, 528 (1992).
8. These cells form a subset of those used in the description of a different drawing task, and the anatomical location of these cells is reported in (7). The task began when a 1.2-mm target circle appeared on the screen. The animal then placed its finger in the circle and held it there for a random period (200 to 600 ms). This circle was located either in the center or at the top of the screen and served as the starting point for a spiral that was drawn from the inside->out or from the outside->in. After the initial hold period, the spiral appeared on the screen and the circle jumped to a new position along the figure. The animal was required to drag its finger to the new location of the circle within 300 ms. Upon acquisition of the target, the target would immediately jump to the next of 40 positions along the figure. In this way the target always stayed ahead of the monkey's finger until the figure was completely drawn. This is not strictly a tracking task, because the animal had full view of the entire figure to be drawn and was free to trace the figure at its own pace provided that it acquired the moving target location within 300 ms. If the animal did not reach the target within this period or if it lifted its finger from the screen, the trial was aborted. After successful completion of the task, the animal was administered a liquid reward.
9. The occurrence times of each action potential were used to obtain a firing rate by breaking the tracing time into 100 bins starting at movement onset. This way of normalizing each trial was done so that corresponding bins from trials of different duration could be added. Population vectors were calculated

$$P_j = \sum_i^{349} w_{ij} C_i$$

for each bin j , C_i is the preferred direction of the i^{th} cell and w_{ij} is a weighting function given by

$$w_{ij} = \frac{d_{ij} - \bar{d}_i}{d_{\text{max}_i} - \bar{d}_i}$$

where d_{ij} is the square root-transformed discharge rate [see note 13 in (3)] for the i^{th} cell in the j^{th} bin, d_{max_i} is the transformed maximum discharge rate for the cell, and \bar{d}_i is the transformed geometric mean discharge rate of the cell. Breaking the data into 100 bins resulted in 100 population vectors and 99 velocity vectors. Comparisons between the population and movement vectors were made either by use of a spline function to extrapolate the velocity data to 100 bins or by use of only the first 99 population vectors.

10. The path curvature was calculated by a three-point method as the angle between successive vectors divided by the arc length between the first and last point. An average bin duration was

calculated by taking the mean drawing time and dividing by the number of bins. Angular velocity in each bin was taken as the change in direction divided by the average bin duration. A polynomial equation with four coefficients ("Poly_Fit," PV-WAVE software from Visual Numerics Inc.) was used to fit the population and movement directions and magnitudes with a least-squared error.

11. A. Lundberg, *Exp. Brain Res.* 12, 317 (1971); G. M. Edelman and V. B. Mountcastle, *The Mindful Brain* (MIT Press, Cambridge, MA, 1978); J. F. Kalaska and D. J. Crammond, *Science* 255, 1517 (1992); K. V. Bae, V. B. Esipenko, Y. P. Shimansky, *Neuroscience* 43, 237 (1991); G. Wittenberg and W. B. Kristan, *J. Neurophysiol.* 68, 1693 (1992); S. R. Lockery and W. B. Kristan, *J. Neurosci.* 10, 1811 (1990); M. W. Jung and B. L. McNaughton, *Hippocampus* 3, 165 (1993).
12. I thank A. Kakavand for training the animals. A. Kakavand and J. L. Adams assisted in the experiments. Supported by the National Institutes of Health (grant NS-26375).

8 March 1994; accepted 25 May 1994

Endothelial NOS and the Blockade of LTP by NOS Inhibitors in Mice Lacking Neuronal NOS

Thomas J. O'Dell,* Paul L. Huang, Ted M. Dawson, Jay L. Dinerman, Solomon H. Snyder, Eric R. Kandel,† Mark C. Fishman

Long-term potentiation (LTP) is a persistent increase in synaptic strength implicated in certain forms of learning and memory. In the CA1 region of the hippocampus, LTP is thought to involve the release of one or more retrograde messengers from the postsynaptic cell that act on the presynaptic terminal to enhance transmitter release. One candidate retrograde messenger is the membrane-permeant gas nitric oxide (NO), which in the brain is released after activation of the neuronal-specific NO synthase isoform (nNOS). To assess the importance of NO in hippocampal synaptic plasticity, LTP was examined in mice where the gene encoding nNOS was disrupted by gene targeting. In nNOS⁻ mice, LTP induced by weak intensity tetanic stimulation was normal except for a slight reduction in comparison to that in wild-type mice and was blocked by NOS inhibitors, just as it was in wild-type mice. Immunocytochemical studies indicate that in the nNOS⁻ mice as in wild-type mice, the endothelial form of NOS (eNOS) is expressed in CA1 neurons. These findings suggest that eNOS, rather than nNOS, generates NO within the postsynaptic cell during LTP.

Although the induction of LTP in the CA1 region of the hippocampus occurs postsynaptically, presynaptic changes are

thought to also contribute to the enhancement of synaptic strength (1). Thus, LTP at these synapses requires the release of a retrograde messenger that acts on the presynaptic terminals to increase transmitter release (2). A likely candidate retrograde messenger is NO (3), a membrane-permeant gas generated by the enzyme NOS (4). There are several isoforms of NOS that fall into two major classes: (i) inducible NOS present in macrophages and (ii) constitutive Ca²⁺-regulated NOS, which includes two isoforms, endothelial (eNOS) and neuronal (nNOS) (5).

A number of observations are consistent with the possibility that NO is a retrograde messenger for LTP and that it is generated by a constitutive Ca²⁺-regulated isoform, presumably the neuronal isoform (3). Acti-

T. J. O'Dell and E. R. Kandel, Howard Hughes Medical Institute and Center for Neurobiology and Behavior, College of Physicians and Surgeons of Columbia University, New York, NY 10032, USA.

P. L. Huang and M. C. Fishman, Cardiovascular Research Center, Massachusetts General Hospital East and Harvard Medical School, Charlestown, MA 02129, USA.

T. M. Dawson, Department of Neurology and Department of Neuroscience, Johns Hopkins University Medical School, Baltimore, MD 21205, USA.

J. L. Dinerman and S. H. Snyder, Department of Neuroscience and Department of Medicine, Cardiology Division, Johns Hopkins University Medical School, Baltimore, MD 21205, USA.

*Present address: Department of Physiology, University of California at Los Angeles School of Medicine, Los Angeles, CA 90024, USA.

†To whom correspondence should be addressed.

vation of the *N*-methyl-D-aspartate receptor by glutamate and the influx of Ca^{2+} is required for the induction of LTP (6), and this Ca^{2+} influx activates NOS in the brain (7). Inhibitors of NOS block LTP (8–10) and do so even when injected into the postsynaptic CA1 pyramidal cell from which LTP is induced (9, 10). Hemoglobin, a large protein that is not taken up into cells, has a porphyrin ring that avidly binds NO and blocks LTP when perfused extracellularly (9, 10). Finally, application of exogenous NO produces an activity-dependent enhancement of synaptic transmission that resembles LTP (11).

A necessary requirement for the putative role of NO as a retrograde messenger in LTP would be the localization of NOS to CA1 pyramidal cells. However, CA1 pyramidal cells do not express nNOS mRNA (4, 12, 13), although they show weak immunocytochemical staining for NOS (14). Moreover, inhibitors of NOS do not block LTP under all circumstances (15, 16). Finally, carbon monoxide (CO), another freely diffusible gas, simulates the properties of NO as a retrograde messenger, and inhibitors of heme oxygenase, the enzyme that generates CO and is localized to pyramidal cells (17), also block LTP (11, 18). Thus, it is not clear whether the neuronal form of NOS generates NO in CA1 pyramidal cells or even whether NO

functions as a retrograde messenger during the induction of LTP (2, 6). We here have begun to address these questions directly using mice with null mutations in the gene encoding neuronal NOS (19).

In mice with such mutations in the nNOS gene generated by homologous recombination, both nNOS mRNA and protein are completely absent. These mice appear to have no gross structural abnormalities within the central nervous system, including the hippocampus (19). In addition, excitatory synaptic transmission in the CA1 region of hippocampal slices from nNOS⁻ mice is normal (20). In these mice, the maximal amplitude of field excitatory postsynaptic potentials (EPSPs) was comparable to that seen in slices from wild-type animals (wild-type, 8.71 ± 0.38 mV, $n = 18$ animals, 90 slices; nNOS⁻, 9.01 ± 0.41 mV, $n = 18$ animals, 90 slices). Similarly, paired-pulse facilitation, a presynaptic form of synaptic plasticity of short duration, was similar in both nNOS⁻ and wild-type mice (Fig. 1).

To determine whether disruption of the gene encoding nNOS impairs hippocampal LTP, we compared the amount of LTP generated in slices from nNOS⁻ mice and from wild-type controls using an induction protocol for LTP known to be sensitive to

inhibitors of NOS (10). LTP was induced with two 1-s-long trains of 100-Hz stimulation at weak stimulus intensity. With this protocol, the amount of LTP evident in the mutant 1 hour after the tetanus was only slightly smaller (a reduction of 25%) than that seen in wild-type controls (Fig. 2A). In wild-type slices, the excitatory synaptic potentials were enhanced to $148 \pm 13.6\%$ of pre-tetanus control levels 60 min after the tetanus ($n =$ five animals, seven slices), whereas in slices from nNOS⁻ mice the EPSPs were $135.8 \pm 10.5\%$ of those of the pre-tetanus control ($n =$ six animals, eight slices). Although with this sample size this difference was not statistically significant ($t[9] = 0.745$, not significant), each of the 50 responses after the tetanus was slightly smaller in the NOS⁻ mice than in the wild-type mice.

The effectiveness of NOS inhibitors in blocking LTP seems to depend on the stimulation protocol used to induce LTP (15, 16) (Fig. 3). In particular, inhibitors of NOS do not block LTP when it is maximally induced by a strong tetanic stimulation (15, 16). Accordingly, one might predict that even the small difference noted at weaker intensities would disappear with strong stimulation. Indeed, with two trains of 100-Hz stimulation at a strong intensity,

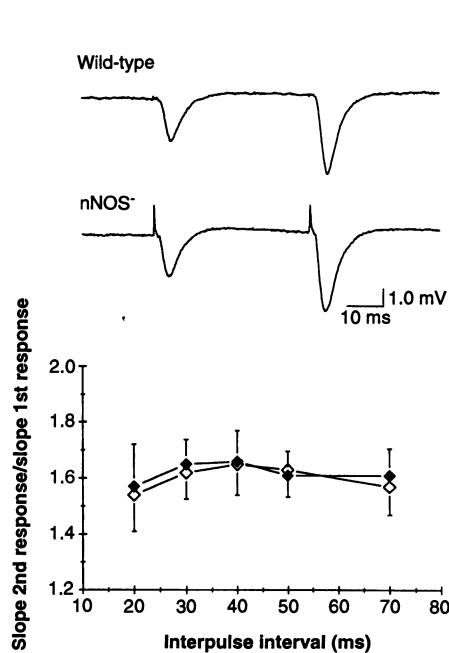


Fig. 1. Paired-pulse facilitation is not altered in nNOS⁻ mice. Pairs of stimulation pulses were delivered at interpulse intervals of 20, 30, 40, 50, and 70 ms. Points are mean \pm SEM, $n = 7$ animals, 19 slices for wild-type mice (solid symbols) and 7 animals, 22 slices for nNOS⁻ mice (open symbols). Traces at the top show typical paired-pulse facilitation (50-ms interval) in slices from a wild-type mouse (top) and an nNOS⁻ mouse (bottom).

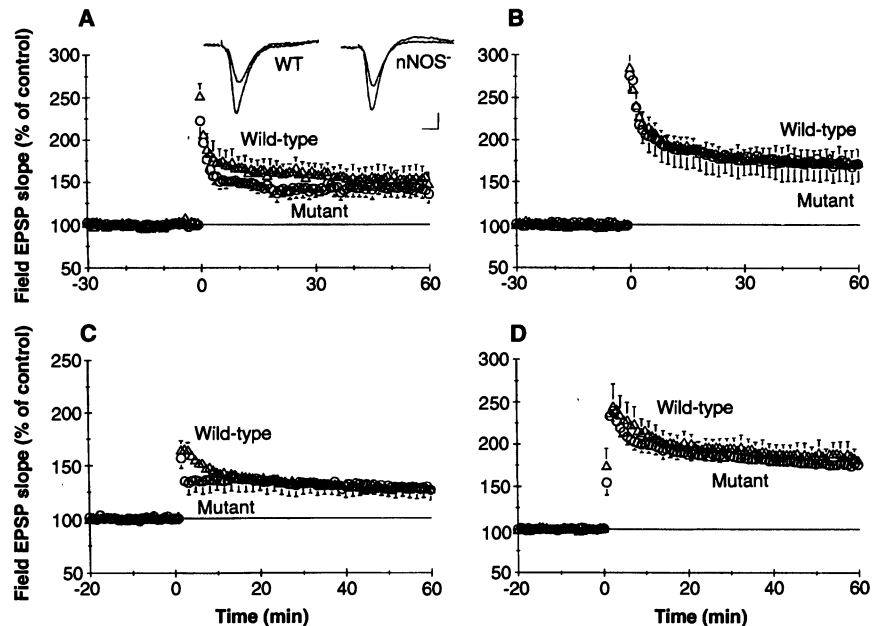


Fig. 2. Long-term potentiation is normal in slices from nNOS⁻ mice. (A and B) After 30 min of baseline synaptic transmission was recorded, LTP was induced with two trains of 100-Hz stimulation delivered at either a weak (A) or strong (B) stimulation intensity. Both protocols produced LTP in slices from wild-type (triangles) and nNOS⁻ (circles) mice. Insets in (A) show typical responses recorded before and 60 min after LTP induction (larger response) in slices from both wild-type and nNOS⁻ mice. Scale bars are 1 mV and 5 ms. (C and D) Long-term potentiation induced with theta-burst stimulation protocols applied at either weak (C) or strong (D) stimulation intensity was also normal in slices from nNOS⁻ mice. Although the amount of potentiation measured 60 min after weak theta-burst stimulation in slices from nNOS⁻ mice was equal to that seen in slices from wild-type animals, the amount of enhancement shortly after theta-burst stimulation (first 3 min) was smaller in slices from nNOS⁻ mice. Baseline is indicated by the horizontal line.

there was, in fact, no difference between nNOS⁻ and control mice 60 min after the tetanus (wild-type mice, 172.8 ± 16.5% of the pre-tetanus control, n = six animals, eight slices; nNOS⁻ mice, 171 ± 20.8% of the pre-tetanus control, n = six animals, eight slices; *t*[10] = 0.0496, not significant) (Fig. 2B).

We explored the effects of weak stimuli further using a theta-burst protocol (20) that approximates normal, physiological patterns of synaptic activity in the hippocampus (21). This potentiation is blocked fully by NOS inhibitors (22). When theta-burst stimulation was delivered at a weak intensity (Fig. 2C), a small but similar amount of LTP was generated in slices from wild-type and from nNOS⁻ animals (23). However, the enhancement of EPSPs during the first 3 min after theta-burst stimulation was significantly smaller (*P* < 0.05) in nNOS⁻ mice compared to that in wild-type mice. At a stronger intensity, theta-burst stimulation produces very large LTP (Fig. 2D), yet here again the amount of potentiation in nNOS⁻ mice is similar to that in wild-type mice (23). These results indicate that the neuronal-specific isoform of NOS is not essential for LTP in the CA1 region of the hippocampus. Nevertheless, this isoform seems to play a minor role in the first few minutes when LTP is induced with weak intensity theta-burst stimulation.

In light of previous work reporting a blockade of LTP by inhibitors of NOS (8–10, 15, 16), our observations that hippocampal synaptic plasticity is essentially normal in nNOS⁻ mice were surprising (24) and could result from compensatory changes in pathways leading to the generation of other retrograde messenger molecules such as CO (11, 17, 18). We therefore examined the effects of NOS inhibitors on LTP in slices from wild-type and nNOS⁻ mice. Because the effects of NOS inhibitors on LTP depend on the tetanus protocol used to induce LTP (15, 16), we examined the effect of *N*-nitro-arginine (NOARG) on LTP using both the weak and strong theta-burst stimulation protocols. In both wild-type and nNOS⁻ mice, these protocols produced both the smallest and the largest degree of potentiation (Fig. 2, C and D). In slices from wild-type animals, 100 μM NOARG completely blocked the LTP induced by the weak theta-burst stimulation protocol (*t*[13] = 2.495, *P* < 0.05). The EPSPs were reduced to 101.4 ± 7.2% of the baseline (n = four animals, nine slices) in slices treated with NOARG when measured 60 min after theta-burst stimulation (Fig. 3A). By contrast, this NOS inhibitor had no effect on LTP produced by strong theta-burst stimulation. Thus, the amount of LTP in wild-type slices

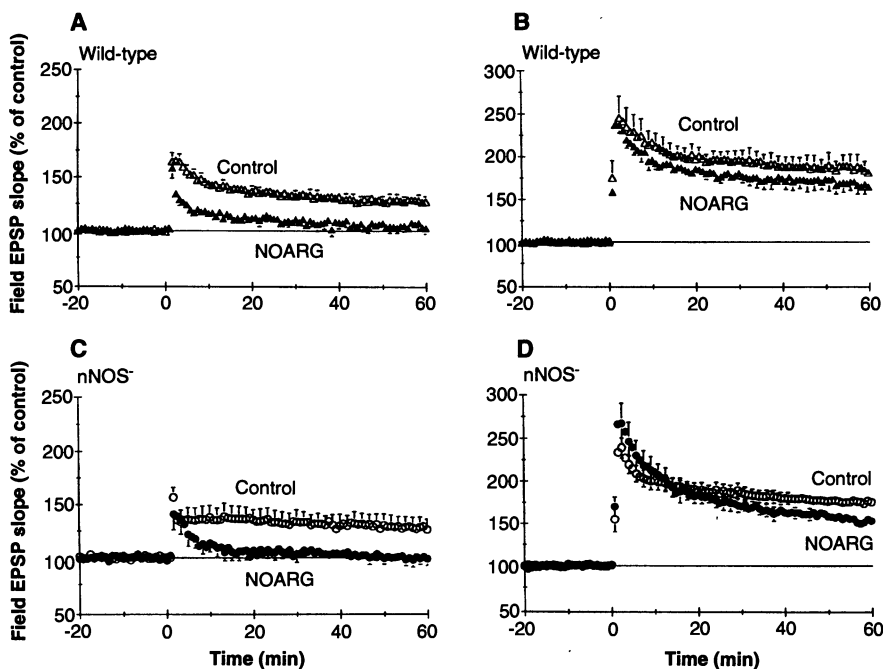


Fig. 3. Effect of the NOS inhibitor NOARG on LTP induced by weak, but not strong, theta-burst stimulation in both wild-type and nNOS⁻ mice. NOARG (100 μM) was applied for 1 to 3 hours before theta-burst stimulation and was present throughout. (A) In wild-type slices, NOARG completely blocked LTP induced by weak theta-burst stimulation. (EPSPs 60 min after theta-burst stimulation were not significantly larger than before theta-burst stimulation; *t*[3] = 0.197, not significant). (B) Strong theta-burst stimulation induced significant LTP (*t*[5] = 7.1367, *P* < 0.01) even in the presence of NOARG. (C) In nNOS⁻ hippocampal slices, LTP induced with weak theta-burst stimulation was blocked by NOARG (60 min after weak theta-burst stimulation in NOARG, EPSPs were not significantly enhanced above the baseline; *t*[3] = 0.531, not significant). (D) In slices from nNOS⁻ mice, strong theta-burst stimulation in the presence of NOARG induces LTP. (EPSPs 60 min after theta-burst stimulation were significantly enhanced compared to baseline EPSPs before theta-burst stimulation; *t*[2] = 8.703, *P* < 0.01.) Baseline is indicated by the horizontal line.

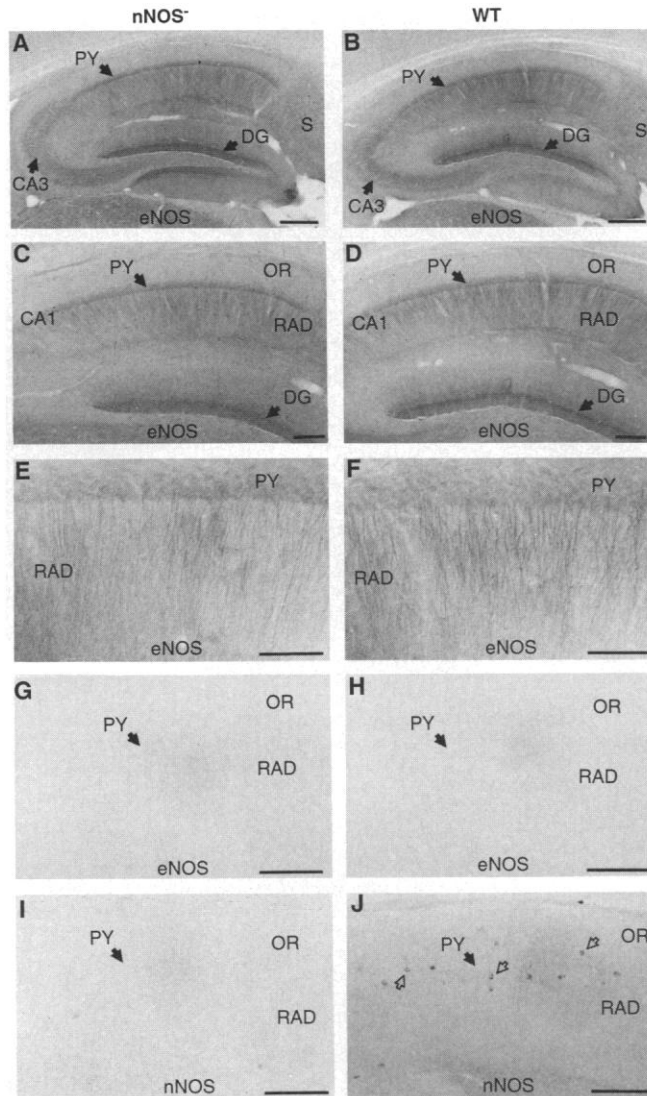
exposed to NOARG (167 ± 12.4% of baseline, n = four animals, eight slices) was not significantly less than that observed in control experiments when measured 60 min after theta-burst stimulation (*t*[8] = 0.92, not significant) (Fig. 3B).

We repeated these two protocols in slices from nNOS⁻ mice. Despite the fact that the neuronal NOS isoform is absent in these mice, the inhibitor of NOS still produced the same pattern of effects on LTP (Fig. 3, C and D). LTP induced with the weak theta-burst stimulation protocol was completely blocked by NOARG (*t*[10] = 2.194, *P* < 0.05) at 60 min after induction by the theta-burst protocol. The EPSPs were 96.8 ± 6.04% of the baseline (n = four animals, seven slices). By contrast, as with wild-type mice the LTP produced by the strong theta-burst protocol in nNOS⁻ mice was not affected by NOARG; 60 min after theta-burst stimulation, the EPSPs were 152.8 ± 6.1% of the baseline (n = three animals, six slices). Thus, even in animals without a functional gene encoding nNOS, NOS inhibitors blocked LTP. Moreover, they did so only when the potentiation was induced by relatively weak stimuli, as in wild-type mice.

These effects of NOS inhibitors on LTP might reflect a nonselective or indirect effect on synaptic transmission or neuronal excitability (22, 25). However, fairly extensive evidence indicates that inhibitors of NOS are specific (26). Moreover, we observed that LTP in both wild-type and nNOS⁻ hippocampal slices is blocked by hemoglobin, an inhibitor of NO signaling that acts by a different mechanism than NOARG (27). Thus, blockade by NOS inhibitors of LTP in nNOS⁻ mice is perhaps more consistent with the possibility that another isoform of NOS may be present in the brains of these mice; this isoform may be responsible for generating NO during the induction of LTP in response to weak stimuli.

Two recent findings are consistent with the presence of another NOS isoform in the brain. First, there is residual NOS activity in the hippocampus of the nNOS⁻ mouse (19). Second, the endothelial form of NOS, once thought to be present only in endothelial cells and to be absent from neurons in the brain, has now been found to be expressed in the brains of wild-type animals and to be specifically present in large amounts in the pyramidal cells of the CA1 region (13). We there-

Fig. 4. Hippocampal CA1 pyramidal neurons are enriched in eNOS in both nNOS⁻ and wild-type (WT) mice. (A) eNOS immunoreactivity in nNOS⁻ mice. (B) eNOS immunoreactivity in wild-type mice. (C) Medium-power view of eNOS immunoreactivity in nNOS⁻ mice. (D) Medium-power view of eNOS immunoreactivity in wild-type mice. (E) High-power view of eNOS immunoreactivity in nNOS⁻ mice. (F) High-power view of eNOS in wild-type mice. (G) Preadsorption with excess eNOS peptide completely eliminates eNOS staining in nNOS⁻ mice. (H) Preadsorption with excess eNOS peptide completely eliminates eNOS staining in wild-type mice. (I) nNOS immunoreactivity is completely absent in nNOS⁻ mice. Preadsorption with excess fusion protein completely eliminates staining for nNOS in wild-type animals (not shown). (J) nNOS immunoreactivity is localized to interneurons (open arrows) of the CA1 region of wild-type mice. The pyramidal cell layer is devoid of nNOS immunoreactivity. DG, dentate gyrus; eNOS, endothelial nitric oxide synthase; nNOS, neuronal nitric oxide synthase; OR, stratum oriens; PY, pyramidal cell layer of CA1; RAD, stratum radiatum; S, subiculum. Bar = 150 μ m in (A) and (B); 100 μ m in (C) and (D); and 50 μ m in (E) through (J).



fore wondered whether eNOS was also enriched in CA1 pyramidal cells of nNOS⁻ mice. Immunostaining with a selective eNOS antibody revealed that eNOS is enriched in the CA1 pyramidal regions of the hippocampi in nNOS⁻ mice, as it is in wild-type animals (Fig. 4) (13). Staining is concentrated within the pyramidal cell body and dendritic processes. This staining contrasts with nNOS immunostaining, which is absent in nNOS⁻ mice with this antibody and is localized only to interneurons of the CA1 pyramidal region of wild-type mice (Fig. 4) (13). Although eNOS and nNOS are enzymatically similar and share cofactor requirements, the endothelial form is myristoylated and membrane-associated, whereas nNOS is soluble. Membrane localization might enhance the precision of spatial signaling, relevant both to LTP and to other potential roles of NO in the brain.

Thus, using a combined genetic, physiologic, and immunologic approach, we were

able to clarify three previously conflicting issues concerning the role of NO as a retrograde signal. First, our data suggest that the endothelial rather than the neuronal isoform of NOS is the major source of NO in the postsynaptic cell. If this source of NO is essential for generating a retrograde signal for LTP, ablation of the eNOS isoform should abolish LTP induced by weak-intensity stimulation protocols. Second, our results as well as those of others (15), demonstrating that maximal LTP induced by high-intensity stimulation is not blocked by inhibitors that affect both eNOS and nNOS, may explain earlier failures to block LTP with inhibitors of NOS. Third, the failure to block maximal LTP with inhibitors of NOS suggests further that even if NO proved critical for LTP produced with weak stimulation, additional retrograde messengers, such as CO (11, 18), platelet-activating factor (28), or arachidonic acid (2, 10), are likely to be required for maximal LTP

produced with strong intensities of stimulation. Consistent with this possibility, inhibitors of heme oxygenase inhibit even maximal LTP produced by maximal intensities of stimuli (11).

REFERENCES AND NOTES

1. J. M. Bekkers and C. F. Stevens, *Nature* **346**, 724 (1990); R. Malinow and R. W. Tsien, *ibid.*, p. 177; A. Larkman, T. Hannay, K. Stratford, J. Jack, *ibid.* **360**, 70 (1992); D. M. Kullmann and R. A. Nicoll, *ibid.* **357**, 240 (1992).
2. J. H. Williams, M. L. Errington, Y.-G. Li, M. A. Lynch, T. V. P. Bliss, *Sem. Neurosci.* **5**, 149 (1993).
3. J. A. Gally, P. R. Montague, G. N. Reeke, G. M. Edelman, *Proc. Natl. Acad. Sci. U.S.A.* **87**, 3547 (1990); E. M. Schuman and D. V. Madison, *Sem. Neurosci.* **5**, 207 (1993).
4. D. S. Bredt and S. H. Snyder, *Neuron* **8**, 3 (1992); D. S. Bredt, P. M. Hwang, S. H. Snyder, *Nature* **347**, 768 (1990); D. S. Bredt *et al.*, *Neuron* **7**, 615 (1991).
5. C. Nathan, *FASEB J.* **3**, 31 (1992); S. Moncada and A. Higgs, *N. Engl. J. Med.* **329**, 2002 (1993); D. S. Bredt and S. H. Snyder, *Annu. Rev. Biochem.* **63**, 175 (1994).
6. T. V. P. Bliss and G. L. Collingridge, *Nature* **361**, 31 (1993).
7. J. Garthwaite, S. L. Charles, R. Chess-Williams, *ibid.* **336**, 385 (1988); S. J. East and J. Garthwaite, *Neurosci. Lett.* **123**, 17 (1991); D. S. Bredt and S. H. Snyder, *Proc. Natl. Acad. Sci. U.S.A.* **86**, 9030 (1989).
8. G. A. Bohme, C. Bon, J. M. Stutzmann, A. Doble, J. C. Blanchard, *Eur. J. Pharmacol.* **199**, 379 (1991); C. Bon, G. A. Bohme, A. Doble, J. M. Stutzmann, J. C. Blanchard, *Eur. J. Neurosci.* **4**, 420 (1992); J. E. Haley, G. L. Wilcox, P. F. Chapman, *Neuron* **8**, 211 (1992).
9. E. M. Schuman and D. V. Madison, *Science* **254**, 1503 (1991); *ibid.* **263**, 532 (1994).
10. T. J. O'Dell, R. D. Hawkins, E. R. Kandel, O. Arancio, *Proc. Natl. Acad. Sci. U.S.A.* **88**, 11285 (1991).
11. M. Zhuo, S. A. Small, E. R. Kandel, R. D. Hawkins, *Science* **260**, 1946 (1993).
12. H. H. Schmidt *et al.*, *J. Histochem. Cytochem.* **90**, 1439 (1992).
13. J. L. Dinerman, T. M. Dawson, M. J. Schell, A. Snowman, S. H. Snyder, *Proc. Natl. Acad. Sci. U.S.A.* **91**, 4214 (1994).
14. F. E. Schweizer *et al.*, *Soc. Neurosci. Abstr.* **19**, 241 (1993).
15. D. M. Chetkovich, E. Klann, J. D. Sweatt, *NeuroReport* **4**, 919 (1993); J. E. Haley, P. Malen, P. F. Chapman, *Neurosci. Lett.* **160**, 85 (1993).
16. V. K. Gribkoff and J. T. Lum-Ragan, *J. Neurophysiol.* **68**, 639 (1992); J. T. Lum-Ragan and V. K. Gribkoff, *Neuroscience* **57**, 973 (1993); J. H. Williams *et al.*, *Neuron* **11**, 877 (1993).
17. A. Verma, D. J. Hirsch, C. E. Glatt, G. V. Ronnett, S. H. Snyder, *Science* **259**, 381 (1993).
18. C. F. Stevens and Y. Wang, *Nature* **364**, 147 (1993).
19. P. L. Huang, T. M. Dawson, D. S. Bredt, S. H. Snyder, M. C. Fishman, *Cell* **75**, 1273 (1993).
20. Slices of mouse hippocampus (400 μ m thick) were prepared [S. G. N. Grant *et al.*, *Science* **258**, 1903 (1992)] and maintained at 30°C in an interface chamber. The recording chamber was perfused (1 to 3 ml/min) with an artificial cerebrospinal fluid (ACSF) containing 124 mM NaCl, 4.4 mM KCl, 25 mM NaHCO₃, 1.0 mM Na₂H₂PO₄, 2.0 mM CaCl₂, 2.0 mM MgSO₄, and 10 mM glucose. Slices were allowed to recover from slice preparation for at least 1.5 hours before electrophysiological recordings. Field EPSPs were recorded with an extracellular electrode (filled with ACSF; resistance = 5 to 10 megohms) placed in the stratum radiatum of the CA1. Schaffer collateral-commissural fibers in the stratum radiatum were stimulated at 0.02 Hz with a nickel-chromium wire

stimulating electrode that was bipolar and coated with Formvar (AM-Systems). Before each experiment, we determined the maximal EPSP amplitude by increasing the stimulation intensity in small increments until the amplitude of the peak of the negative extracellular potential saturated. The opposing effects of the positive population spike recorded in the stratum radiatum at high stimulation intensities were not taken into account. The strength of presynaptic fiber stimulation was then adjusted to evoke EPSPs that were 25% of the maximal amplitude. After recording baseline synaptic responses for 20 to 30 min, we induced LTP using one of four different protocols. Two of these protocols consisted of two trains of 100-Hz stimulation (1.0-s duration) delivered 20 s apart. For weak intensity 100-Hz stimulation, the stimulation intensity was left at that used to evoke baseline synaptic responses. For strong intensity 100-Hz stimulation, the 100-Hz trains were delivered at a stimulation intensity sufficient to evoke EPSPs that were 75% of the maximal EPSP amplitude. LTP was also induced by theta-burst stimulation protocols that consisted of bursts of four stimulation pulses at 100 Hz delivered with 200 ms between each burst (that is, at 5 Hz). Weak theta-burst stimulation consisted of 25 bursts given at baseline stimulation intensity, whereas strong theta-burst stimulation consisted of 10 bursts delivered at an intensity sufficient to evoke EPSPs that were 50% of the maximal obtainable EPSP amplitude. As controls, age-matched littermates with intact NOS alleles, as well as 129/Sv and C57BL/6 (male and female) mice, were used. The animals ranged from approximately 6 to 23 weeks of age. The results from wild-type mice of different genetic backgrounds and sex were similar, and the results were combined. All values reported are mean \pm SEM. We performed statistical comparisons by using Student's *t* tests for two independent means. For immunostaining, nNOS⁻ and wild-type mice were anesthetized with pentobarbital (100 mg per kilogram of body weight) and killed by perfusion with phosphate-buffered saline, which was followed by perfusion with freshly depolymerized 4% paraformaldehyde (PF) in 0.1

M phosphate buffer (PB). The brains were removed and postfixed in 4% PF in PB for 2 to 4 hours. The brains were then cryoprotected by soaking overnight in 20% (v/v) glycerol in PB. Immunostaining for eNOS and nNOS was performed as described (13). Free-floating tissue sections (40 μ m) were incubated in affinity-purified eNOS antiserum (1:50 dilution) or affinity-purified nNOS antiserum (1:1000 dilution). Staining was visualized with an avidin-biotin-peroxidase system (Vector Laboratories) with diaminobenzidine as a chromagen. Controls for specific staining included preadsorption with excess peptide for eNOS and excess fusion protein (amino acids 1 to 181 of cloned nNOS) for nNOS, which completely eliminated staining for the antisera.

21. J. Larson, D. Wong, G. Lynch, *Brain Res.* **368**, 347 (1986).
22. W. Y. Musleh, K. Shahi, M. Baudry, *Synapse* **13**, 370 (1993).
23. In slices from wild-type animals, 60 min after weak theta-burst stimulation EPSPs were $126.2 \pm 5.5\%$ of the baseline ($n = 11$ animals, 19 slices); EPSPs were $184.2 \pm 11.8\%$ of the baseline ($n = 6$ animals, 10 slices) after strong theta-burst stimulation. In nNOS⁻ slices, EPSPs measured 60 min after weak and strong theta-burst stimulation were $127.4 \pm 8.9\%$ ($n = 8$ animals, 14 slices) and $176.1 \pm 5.2\%$ ($n = 6$ animals, 13 slices) of the baseline, respectively. For both theta-burst stimulation protocols, the amount of LTP in slices from nNOS⁻ animals was not significantly different from that seen in slices from wild-type animals (weak stimulation: $t[17] = 0.11$, not significant; strong stimulation: $t[10] = 0.631$, not significant).
24. We also observed that homosynaptic long-term depression (LTD) was normal in slices from nNOS⁻ mice. In these experiments, LTD was induced in hippocampal slices obtained from young animals (4 to 6 weeks old) by 900 pulses of 1-Hz stimulation. One hour after beginning 1-Hz stimulation, EPSPs were $84.2 \pm 4.5\%$ of the pre-1 Hz baseline ($n = 6$ animals, 11 slices) in wild-type slices and $85.1 \pm 4.6\%$ of the baseline ($n = 5$ animals, 10 slices) in nNOS⁻ slices.

25. Y. Izumi, D. B. Clifford, C. F. Zorumski, *Science* **257**, 1273 (1992).
26. E. S. Furtine, M. F. Harmon, J. E. Paith, E. P. Garvey, *Biochemistry* **32**, 8512 (1993); R. G. Knowles and S. Moncada, *Biochem. J.* **298**, 249 (1994).
27. In wild-type hippocampal slices that were continuously bathed in 50 μ M oxyhemoglobin (beginning at least 1.5 hours before induction of LTP was attempted), EPSPs 60 min after weak theta-burst stimulation were $98.89 \pm 4.2\%$ of the baseline ($n =$ three animals, six slices; not significantly different from the baseline, $t(2) = 0.46$, not significant). LTP in slices from nNOS⁻ mice was also blocked by oxyhemoglobin. EPSPs 60 min after weak theta-burst stimulation were $98.43 \pm 3.62\%$ of the baseline ($n =$ three animals, six slices) and not significantly different from pre-theta-burst stimulation levels [$t(2) = 0.434$, not significant]. Importantly, the effects of hemoglobin on LTP may be due to its ability to bind extracellular CO, another candidate retrograde messenger, and thus to prevent it from reaching the presynaptic terminal.
28. A. Arai and G. Lynch, *Eur. J. Neurosci.* **4**, 411 (1992); G. D. Clark, L. T. Happel, C. F. Zorumski, N. G. Bazan, *Neuron* **9**, 1211 (1992); A. Wieraszko, G. Li, E. Kordecki, M. V. Hogan, Y. H. Ehrlich, *ibid.* **10**, 553 (1993); K. Kato, G. D. Clark, N. G. Bazan, C. F. Zorumski, *Nature* **367**, 175 (1994).
29. E.R.K. is a Senior Investigator and T.J.O. is a Research Associate of the Howard Hughes Medical Institute. E.R.K. and T.J.O. were also supported by National Institute of Mental Health grant MH-45923. S.H.S. is supported by U.S. Public Health Service grants DA-00266, Research Scientist Award DA-00074, and a grant from the William M. Keck Jr. Foundation. T.M.D. is supported by U.S. Public Health Service grant CIDA NS-01578. P.L.H. and M.C.F. are supported by NIH and a sponsored research agreement with Bristol-Myers Squibb.

18 February 1994; accepted 2 June 1994

TECHNICAL COMMENTS

Cortical Reorganization and Deafferentation in Adult Macaques

Until 1991, there was a general consensus that the reorganization of the body map in the primary sensory cortex after deafferentation in adult animals only occurs within 1 to 2 mm of neurons with normal receptive fields (1). In addition to the immediate effects of deafferentation, such as the unmasking of existing excitatory inputs from adjacent body parts (2), changes to the deafferented part of the map continue over weeks or months (3). However, most evidence suggests that plasticity is limited to a zone no wider than the extent of the arbors of thalamocortical axons (1). This reinforces the notion (the "unmasking hypothesis") that most of the reorganization occurs through an increase in the efficacy of thalamocortical connections that existed before deafferentation (4).

The evidence for limited ability of the

adult cortex to reorganize was challenged by T. P. Pons and his colleagues (5), who made extracellular microelectrode recordings from neurons in the primary sensory area of the postcentral gyrus of anesthetized adult macaque monkeys more than 12 years after unilateral or bilateral sectioning of the dorsal roots from C2-T4. In the zone within which the arm and hand would normally be represented, Pons *et al.* found that all neurons now had receptive fields on the lower face, as if the entire strip of cortex below the hand area, in which the lower jaw is represented in intact monkeys, had been stretched out over a sheet of deafferented cortex that was 10 to 14 mm long (5).

We tested a more parsimonious explanation for the results of Pons *et al.* (5). If there were a second representation of the face medial to the arm area, then facial inputs

could take over the deafferented cortex from two fronts. There is evidence that the lateral parts of the face and the lower jaw are represented a second time in the "upper head area." This region was originally discovered at the dorsal end of the arm representation by Woolsey *et al.* (6), who used evoked potentials with monkeys. Later, the existence of neurons with tactile receptive fields on the face within the upper head area was established (7, 8). Our experiment, using an awake (N₂O-sedated) adult female macaque monkey (*Macaca mulatta*), was designed to confirm that some neurons in the upper head area have receptive fields on the lower jaw and to measure the distance between the two facial representations (9).

In agreement with earlier work, we found that the medial boundary of the primary face area overlapped that receiving inputs from the thumb (Fig. 1). Facial fields adjacent to those on the thumb were usually found on the lower jaw or lip (Fig. 2), but neurons with receptive fields on the nose and eyebrows were occasionally found next to those on the thumb or fingers (Fig. 2). Similar relationships were reported by